

NASA Technical Memorandum 107328
AIAA-96-2729

Pulsed Plasma Thruster Contamination

Roger M. Myers and Lynn A. Arrington
NYMA, Inc.
Brook Park, Ohio

Eric J. Pencil
Lewis Research Center
Cleveland, Ohio

Justin Carter, Jason Heminger, and Nicolas Gatsonis
Worcester Polytechnic Institute
Worcester, Maine

Prepared for the
32nd Joint Propulsion Conference
cosponsored by AIAA, ASME, SAE, and ASEE
Lake Buena Vista, Florida, July 1-3, 1996



National Aeronautics and
Space Administration

Pulsed Plasma Thruster Contamination

Roger M. Myers¹ and Lynn A. Arrington²
Engineering Services Division
NYMA Inc., NASA Lewis Research Center
Brookpark, OH 44142

Eric J. Pencil³
NASA Lewis Research Center
Cleveland, OH 44135

Justin Carter,⁴ Jason Heminger,⁵ and Nicolas Gatsonis⁶
Worcester Polytechnic Institute
Worcester, MA

Abstract

Pulsed Plasma Thrusters (PPTs) are currently baselined for the Air Force Mightysat II.1 flight in 1999 and are under consideration for a number of other missions for primary propulsion, precision positioning, and attitude control functions. In this work, PPT plumes were characterized to assess their contamination characteristics. Diagnostics included planar and cylindrical Langmuir probes and a large number of collimated quartz contamination sensors. Measurements were made using a LES 8/9 flight PPT at 0.24, 0.39, 0.55, and 1.2 m from the thruster, as well as in the backflow region behind the thruster. Plasma measurements revealed a peak centerline ion density and velocity of $\sim 6 \times 10^{12} \text{ cm}^{-3}$ and 42,000 m/s, respectively. Optical transmittance measurements of the quartz sensors after 2×10^5 pulses showed a rapid decrease in plume contamination with increasing angle from the plume axis, with a barely measurable transmittance decrease in the ultraviolet at 90° . No change in optical properties was detected for sensors in the backflow region.

Introduction

Pulsed plasma thrusters (PPTs) offer the combined benefits of extremely low average electric power requirements (<1 W to over 100 W), high thruster specific impulse ($\geq 1000 \text{ s}$), and system simplicity derived from the use of an inert solid propellant. Potential applications range from orbit insertion and maintenance of small satellites to attitude control for large geostationary communications satellites. Pulsed plasma thrusters are currently baselined for orbit raising on the Air Force Mightysat II.1 spacecraft to be launched in early 1999. They are also under consideration for attitude and fine orbit control for the NASA New Millennium Program's Earth Orbiting 1 and Deep Space 3 missions. Several recent trade studies have shown that PPTs provide significant mission and system benefits over state-of-art propulsion and attitude control systems for a wide range of near-

Earth and deep-space missions.¹⁻³ Some of these missions include optical sensors which are sensitive to contamination from thruster exhaust plumes, forcing a detailed examination of PPT plume impacts.

Pulsed plasma thrusters rely on the Lorentz force generated by an arc passing from anode to cathode and the self-induced magnetic fields to accelerate a small quantity of fluorocarbon-based propellant. As shown schematically in Fig. 1, the thruster system consists of the accelerating electrodes, an energy storage unit, a power conditioning unit, an ignitor supply, and a propellant feed system. The latter consists of a spring which pushes a stick of fluorocarbon against the accelerating electrodes. This is the only moving part in the PPT system. During operation, the energy storage capacitor is first charged to between 1 and 2 kV. The ignitor supply is then activated to generate a low density plasma which permits the energy storage capacitor to discharge across the face of the fluorocarbon propellant. Peak arc current levels are typically between 2 and 15 kA. The high current arc ablates a small quantity of the propellant which is then accelerated downstream, and the arc is extinguished between

^{1,2}Propulsion Specialist, member AIAA

³Aerospace Engineer, member AIAA

^{4,5}Undergraduate Student

⁶Professor of Mechanical Engin., member AIAA

5 and 15 μ sec after discharge initiation. The pulse cycle can then be repeated at a rate compatible with the available spacecraft power and propulsion requirements. Typical operational missions require between 10^6 and 2×10^7 pulses.

While PPTs have been used on several spacecraft, including three Navy NOVA spacecraft,⁴ technology development was discontinued around 1980. Recent developments in both energy storage and power conditioning technologies provide several options which can result in a system mass reduction by a factor of two while simultaneously doubling the total impulse capability. The NASA PPT program was initiated in 1993 and is currently funding the development of a flight-type system, evaluating critical spacecraft interfaces such as contamination and electromagnetic compatibility, and establishing next-generation flight system requirements. Summaries of recent progress in that effort are given in Refs. 2 and 5 - 7.

PPT contamination arises from the deposition of ablated propellant material on spacecraft surfaces. Potential contaminants include carbon, fluorine, and a range of fluorocarbons. In-flight experience spanning over 10 years of thruster operation on three Navy NOVA spacecraft on which the PPTs fired straight across the solar arrays revealed no conclusive evidence of array degradation traceable to the PPTs.^{4,8} Previous ground-based studies of PPT contamination⁹⁻¹¹ indicate a plume half-angle of approximately 40 degrees, with minimal deposition occurring beyond that angle. While deposition has been measured in the thruster backflow region, it has not been possible to eliminate facility wall scattering as a source for this material.⁹ Facility wall scattering is particularly important for PPTs given their extremely high mass fluxes, which reach several grams per second as a result of the extremely short pulse durations and high instantaneous power levels used in the discharges.¹⁰

The primary objective of this study was to perform preliminary plume assessments and establish techniques for future contamination measurements to be performed using the breadboard PPT being developed at Olin Aerospace under the NASA program. Measurements include transmittance, reflectance, and mass changes for quartz samples placed in both the near- and far-field plumes, and ion current density and velocity distributions in the near-field. Following a brief overview of the experimental apparatus and procedures, the results

of near- and far-field plume measurements will be presented with a discussion of implications for the use of PPTs on spacecraft with sensitive optical instrumentation. Finally a summary of progress to date will be given.

Experimental Apparatus

Pulsed Plasma Thruster

The Lincoln Experimental Satellite (LES) 8/9 thruster was used for all tests reported herein.¹² This thruster has a ~ 20 J energy storage capacitor and is configured to fire automatically at a rate of 2.2 Hz. Its design yields a an impulse bit of 300 μ N-s at a specific impulse of 1000 s and an efficiency near 7%. The ablated mass per pulse ranges from 25 to 33 μ g, with a long term average of 28.5 μ g. This yields, for the measured pulse duration of 12 μ s, an instantaneous mass flow rate of 2.4 g/s - considerably higher than that of most current electric propulsion systems. High mass flow rates lead to high number densities in the plume, which in turn cause enhanced backflow of plume constituents.

As shown schematically in Fig. 2, the LES 8/9 thruster fluorocarbon propellant face is 2.54 cm square, and the electrodes are 2.54 cm long.¹² Two 1.2-cm diameter ignitor plugs are located in the cathode. The LES 8/9 firing circuit alternates between the two plugs to promote more even ablation of the propellant face. Because of the attitude control function for the thruster, the electrodes are rotated 30 $^\circ$ from axial to provide a control moment for the spacecraft. The electrodes are housed in machinable-ceramic exhaust channels. Figure 2 shows that the original thruster exhaust plane is asymmetric in two ways. First, the planar electrode configuration yields two planes of geometric symmetry, parallel and perpendicular to the electrode surfaces. Second, the exhaust channel configuration is different on the anode and cathode sides. On the cathode side the channel extends 2.7 cm beyond the electrode, while on the anode side the channel ends at the electrode tip. The front face of the original system consists of a flat plate with two 5.8-cm by 6.4-cm holes for the two electrode sets. This configuration, which was used for the near-field plume measurements, enhances plume scattering from the cathode side of the chamber and has a pronounced impact on the plume results. Because of this, the far-field tests were performed with the additional exhaust channel extension

shown in Fig. 2. While not perfectly symmetric due to the difference in wall angles on the cathode and anode sides, the channel length with the extension is the same on both cathode and anode sides of the thruster. This configuration is a more accurate approximation of the planned first generation flight-type system from the NASA program.

Test Facilities

Near-field measurements of the LES 8/9 plume were made in a 0.51-m diameter, 0.96-m long bell jar pumped by a 0.25-m diameter oil diffusion pump. The facility base pressure was $\sim 3 \times 10^{-6}$ T, and pressure during operation at 2.2 Hz was $\sim 1 \times 10^{-4}$ T. As shown in Fig. 3, the thruster was mounted on the bottom of the facility facing up, with two diagnostic probe rakes above it.

Far-field plume measurements were made using an 1.52-m diameter, 3.05-m long vacuum facility pumped by an 0.51-m diameter cryopump. The facility base pressure was $\sim 1 \times 10^{-7}$ T, and pressure during thruster operation at 2.2 Hz was $\sim 6 \times 10^{-6}$ T. Facility pressure generally increased gradually during an extended test, sometimes reaching 9×10^{-6} T. The PPT was mounted at the top of the facility pointing down. To reduce the effects of the plume scattering from the bottom of the facility, a baffle consisting of 0.5-m high, 0.05-cm thick, vertical stainless steel plates arranged in a 25-cm by 25-cm squares was placed in the bottom of the facility. As described below, contamination monitors were placed throughout the facility to characterize both the direct impacts of the plume and establish the effects of scattering of the vacuum facility walls.

Diagnostics

Near-Field Measurements:

Near-field measurements were made with sensor rakes mounted at 24- and 39-cm radii from the exit plane. The probe rakes were offset by 10° to prevent the 24 cm rake from shadowing the 39 cm rake. Contamination sensors consisted of 2.0 x 2.0-cm quartz samples placed at the rear of 2.5-cm diameter, 2.5-cm long collimators. The collimators were designed to preclude particles undergoing a single bounce from any surface from reaching the quartz samples. The samples were characterized by their weight, transmittance, and deposited film properties. A spectrometer was used to measure the sample transmittance and reflectance between 350 and 1200 nm. These

measurements represent average values for a 1.0 x 1.8 cm region on the exposed sample. Following exposure to the thruster plume, the samples were reweighed and their optical properties characterized. Weight uncertainty is ± 0.0001 g, and transmittance and reflectance are measured to within 0.5% absolute.

Plume plasma properties were studied using a combination of cylindrical and planar ion current density probes. The cylindrical probes were used for time-of-flight ion velocity measurements. Four 0.32-cm diameter, 1-cm long probes were aligned along the plume centerline perpendicular to the plasma flow at 10 cm intervals. The probes were biased to -40 V. The 2.1-cm diameter planar probes were made of copper and incorporated guard rings to ensure that a one-dimensional sheath approximation could be used. Estimates of secondary electron emission from the copper probe indicate an error of less than 10% from this source. The planar probe and guard ring bias was -40 V.

Far-Field Measurements:

Far-field plume impacts were assessed using collimated quartz samples located in the plume and backflow regions of the thruster. The quartz was characterized in the same fashion as for the near-field measurements. Following the pre-test sample characterization, the samples were installed in 15-cm long, 5.1-cm diameter collimators shown in Fig. 4. Each collimator had two apertures to limit the impact of contaminants bouncing off the collimator walls, resulting in a sample field-of-view of 22.4° . The inner collimator surface was lined with tantalum. This material was not used in the thruster or test facility so contamination due to collimator materials could be readily identified. The collimators were mounted throughout the test facility as shown in Fig. 5, with two 0.55-m semicircular rakes holding four probes each at angles between 40° and 120° from the plume axis, a single collimator located 1.2-m from the thruster 30° off-axis, two collimators in the backflow region, and a single collimator 1.2-m downstream of the thruster facing the bottom of the tank to measure backscatter from the facility walls. The latter collimator was shortened so that its field-of-view was the same as the backflow collimators located behind the thruster. A total of 14 quartz samples were exposed during the test.

Results and Discussion

Near-field

Figure 6 shows the results of the time-of-flight measurements. Plotted are the arrival times of the first peak in the ion current as a function of distance from the thruster exit plane. Ten measurements were made for each probe, and a least-squares fit to the data yielded an ion velocity of 42,000 m/s with an uncertainty of +/- 12%. This ion velocity is consistent with previous measurements made on the a similar thruster.¹³ Figures 7a and b show ion current densities measured 24 cm from the thruster in planes parallel and perpendicular to the electrodes (see Fig. 2). It is apparent that the ion current profile is significantly flatter parallel to the electrodes than perpendicular. Perpendicular to the electrodes the ion current density decreases by a factor of ~ 3.5 within 40° of the axis, whereas parallel to the electrodes it only decreases by ~25%. In both planes the current density decreases by over a factor of 25 within 75° of the thruster axis. These results are consistent with previous data obtained using a PPT having over ten times the energy storage capacity of the LES 8/9 PPT.^{9,14} Using the measured centerline velocities and assuming a singly ionized plume, the peak centerline ion density 24 cm from the thruster is estimated to be ~ $6 \times 10^{12} \text{ cm}^{-3}$. For comparison, this peak density is a factor of 3 - 7 higher than the steady-state density measured in the plumes of 1.4 kW hydrazine arcjets and xenon stationary plasma thrusters currently used on communications satellites.^{15,16} The density drops by over an order of magnitude within 2 μs of the peak value.

Results from the contamination sensors at 24 and 39 cm from the thruster are shown in Fig. 8. Measurements were made with the probes in the plane perpendicular to the PPT electrodes, and the 39 cm sensors were limited to +/- 33° by the test chamber configuration. For angles between -40° and +5° there was net erosion of the quartz, likely resulting from sputtering by the high velocity ions. For positive angles between 5° and 60° there was net deposition, the asymmetry likely resulting from enhanced deposition caused by particles bouncing from the exhaust channel on the cathode side (Fig. 2). Note that the distributions are quite similar for both probe rakes. At 39 cm, however, the maximum erosion/deposition magnitudes are lower and there is a noticeable broadening of the distributions at the larger distance resulting from the plume

expansion. In these tests there was no measurable deposition or erosion beyond - 40° and + 50°.

The composition and structure of the deposited film was examined on the sample which had gained the most weight during testing. Scanning electron microscopy revealed that the film consisted of a base film with a large number of 1 μm and 5 μm particles superimposed on it. Clear evidence of carbon and fluorine was obtained in the overall film and in many of the particles. Additionally, a few particles ~ 5 μm in diameter were found to contain iron, nickel, aluminum and chromium. These could have originated from the PPT electrodes.

Far-field

A 2×10^5 pulse test (25.25 hrs at 2.2 Hz) was conducted over a period of 3 days using the probe rake shown in Fig. 5. This rake has a minimum measurement angle of 30° at 1.2 m from the thruster, and two sensors at 40° (in parallel and perpendicular planes). The test was conducted with the exhaust channel extension to reduce the asymmetries observed in the near-field deposition measurements. Pre- and post-test weight measurements showed no measurable mass gain on any of the samples. This result placed an upper bound of $1.25 \times 10^{-10} \text{ g/cm}^2/\text{pulse}$ on the deposition rate at any of the sample locations. This result is consistent with the near-field measurements, given the angles for which the measurements were made, the increased distances from the thruster to the probes, and the number of pulses in each test.

Optical measurements showed that there was no measurable deposition in the backflow region. Results for all the samples in the backflow region, including those 120° off axis and those behind the thruster facing the tank bottom (backflow 1 and 2 in Fig. 5) are shown in Fig. 9. The noise at 875 nm resulted from a change in optical detector within the spectrometer. There was no measurable difference between the control samples and those exposed to the thruster firing. This is a very important result, as it indicates that, to first order, spacecraft surfaces behind the PPT should not be significantly contaminated by thruster exhaust products. From a facilities standpoint, it appears that very little of the material bouncing from the vacuum facility bottom escapes the baffle to the thruster region.

In the forward area of the plume some transmittance degradation was observed as

expected. Shown in Fig. 10a and b are plots of the transmittance versus wavelength for samples in both the parallel and perpendicular planes between angles of 40° and 90° off the plume axis. The angular dependence of the results was quite striking, with pronounced decreases in transmittance for wavelengths below 800 nm at angles of 40° and 60° from the plume, and a slight decrease below 500 nm at 90° . The transmittance decreased more for samples in the plane perpendicular to the electrodes than for those in the parallel plane. Results for the single sample at 30° , which was 1.2 m from the thruster, are shown in Fig. 11. Again there was a pronounced degradation in transmittance at the lower wavelengths, though the decrease was substantially less than observed with the closer samples.

The potential impact of the deposition on solar arrays was evaluated by calculating the average transmittance between 350 and 1200 nm weighted by the solar irradiance. Results are shown for samples in the parallel and perpendicular planes in Fig. 12. The figure shows that the worst case reduction was less than 0.5% after 2×10^5 pulses for the samples at 40° in the perpendicular plane. For the same angle, the reduction in the plane parallel to the electrodes was less than 0.1%.

The application of PPTs to science missions will require an understanding of PPT plume impacts on optical sensors using limited wavelength ranges. There are three wavelength ranges of primary interest, the astronomical V-band between 505 and 595 nm, the R-band between 590 and 810 nm, and the I-band between 780 and 1020 nm.¹⁵ Average transmittances (not weighted) for these ranges for samples perpendicular to the electrodes are shown in Fig. 13. As expected from the transmittance measurements shown in Fig. 10, the largest decrease is in the V-band, which shows a maximum decrease of 2.5% transmittance at 40° off axis after 2×10^5 pulses. At 90° the decrease is $\sim 0.2\%$, and for the 120° and backflow samples no change is observed. Similar trends, though smaller in magnitude, are seen for the R and I bands. Results for samples parallel to the electrodes show a smaller decrease in transmittance, with a maximum of less than 0.5% in the V-band at 40° .

A major result of this study is the pronounced asymmetry of the plume impacts in the planes parallel and perpendicular to the electrodes.

While not entirely unexpected, previous studies indicated that the degree of asymmetry decreases rapidly away from the thruster, and could be neglected for sample distances comparable to those used in this work. This is clearly not the case, and shows that the orientation of the PPT about the thrust axis can be used to control the deposition of contaminants on surfaces.

Conclusion

Measurements of pulsed plasma thruster plume impacts were made using plasma and contamination diagnostics in both the near- and far-field regions. Results show the plume ion density reaches $\sim 6 \times 10^{12} \text{ cm}^{-3}$ 24 cm from the thruster and that the ion velocity along the centerline is $\sim 42,000 \text{ m/s}$. Contamination studies revealed no measurable deposition in the backflow region, with optical transmittance measurements of collimated quartz samples showing no change after 2×10^5 pulses. This indicates that spacecraft surfaces immediately behind the PPT would not be subject to significant deposition. Contamination measurements forward of the thruster showed that results were sensitive to the configuration of the exhaust channel, and reflect both asymmetries in the channel and the inherent asymmetry resulting from the use of two planar electrodes. Within these constraints, near-field measurements revealed that the high energy ions can result in net sensor erosion within 40° of the thruster axis in the near field region. No mass deposition was measurable for angles larger than 50° . Far-field measurements using samples 0.55 m from the thruster placed in collimators with a 22.4° field of view, located on rakes both parallel and perpendicular to the electrode plane, yielded no measurable weight change for any sample after 2×10^5 pulses, resulting in an upper bound of contaminant deposition of $1.25 \times 10^{-10} \text{ g/cm}^2/\text{pulse}$. Transmittance measurements of these samples showed a significant decrease for samples at 40° and 60° off axis, with a barely measurable decrease at 90° . Integration of these results to obtain the average solar transmittance yielded a maximum decrease of 0.5% in the plane perpendicular to the electrodes and less than 0.1% parallel to the electrodes after 2×10^5 pulses. The observation that no contamination was detectable in the backflow region, and only minor effects were measurable beyond 60° from the thrust axis is very encouraging for the use of PPTs for a wide range of spacecraft applications.

References

- ¹Myers, R. M., Oleson, S., McGuire, M., Meckel, N., and Cassady, R.J., "Pulsed Plasma Thruster Technology for Small Satellite Missions," Proceedings of the 9th AIAA/Utah State University Conference on Small Satellites, Logan, UT, Sept. 1995; see also NASA CR 198427.
- ²Dudzinski, L. A. and Myers, R. M., "Advanced Propulsion Benefits to New Millennium Class Missions," Proceedings of the 9th Annual AIAA/USU Conference on Small Satellites, Logan, UT, Sept. 1995.
- ³McQuire, M. L. and Myers, R.M., "Pulsed Plasma Thrusters for Small Spacecraft Attitude Control," Flight Mechanics/Estimation Theory Symposium, Goddard Space Flight Center, May 13 - 16, 1996.
- ⁴Brill, Y., Eisner, A., and Osborn, L., "The Flight Application of a Pulsed Plasma Microthruster; The NOVA Satellite," AIAA Paper 82-1956, Nov. 1982.
- ⁵Meckel, N., et al., "Improved Pulsed Plasma Thruster for Satellite Propulsion," AIAA Paper 96-2735, July 1996.
- ⁶Kamhawi, H., et al., "Design and Operation of a Laboratory Benchmark PPT," AIAA Paper 96-2732, July 1996.
- ⁷Mikelledes, P. et al., "Modeling of Late-Time Ablation in Teflon Pulsed Plasma Thrusters," AIAA Paper 96-2733, July 1996.
- ⁸Maag, C.R., and Millard, J.M., "Results of the NOVA-3 Contamination Monitoring Equipment," AFAL-TR-87-107, Dec. 1987.
- ⁹Rudolph, L.K. and Jones, R.M., "Pulsed Plasma Thruster Contamination Studied," AIAA Paper 79-2106, Oct. 1979.
- ¹⁰Guman, W.J. and Begun, M., "Pulsed Plasma Thruster Plume Studies," AFRPL-TR-77-2, March 1977.
- ¹¹Dawborn, R. et al., "Operating Characteristics of an Ablative Pulsed Plasma Engine," AFRPL TR-82-17, July 1982.
- ¹²Vondra, R.J., "The MIT Lincoln Laboratory Pulsed Plasma Thruster," AIAA 76-998, November, 1976.
- ¹³Vondra, R.J. et al., "Analysis of Solid Teflon Pulsed Plasma Thruster," J. Spacecraft and Rockets, Vol. 7, No. 12, Dec. 1970, pp. 1402-1406.
- ¹⁴Rudolph, L.K, et al., "Pulsed Plasma Thruster Backflow Characteristics," J. Spacecraft and Rockets, Vol. 17, No. 5, Sept. 1980, pp. 447 - 452.
- ¹⁵Zube, D.M. and Myers, R.M., "Thermal Nonequilibrium in a Low-Power Arcjet Nozzle," J. Propulsion and Power, Vol. 9, No. 4, July-Aug. 1993, pp. 545 - 552.
- ¹⁶Myers, R.M. and Manzella D.H., "Stationary Plasma Thruster Plume Characteristics," IEPC - 93-096, Proceedings of the 23rd International Electric Propulsion Conference, Vol. 2, Sept. 1993.
- ¹⁷Zombeck, M. V., Handbook of Astronomy and Astrophysics, Cambridge University Press, New York, 1990, p. 100.

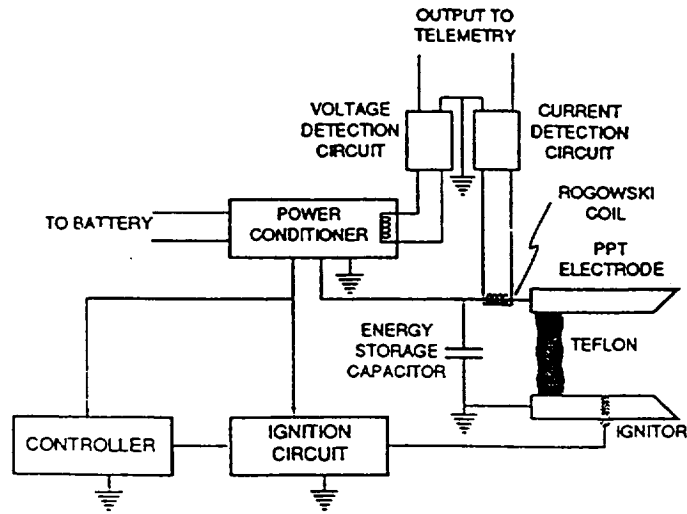


Fig. 1 - PPT flight system schematic. Telemetry signals depend on application.

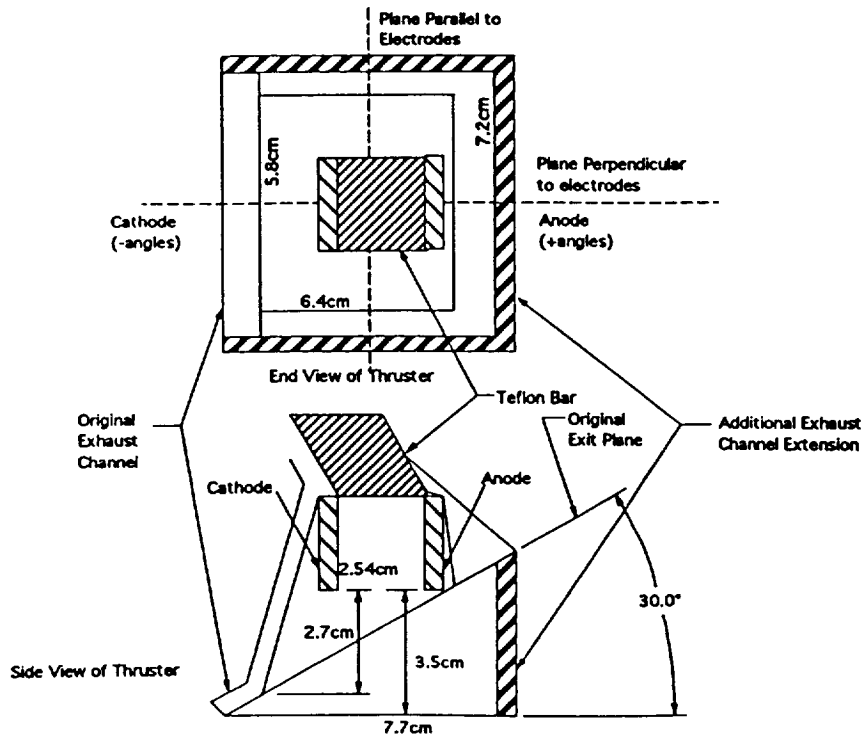


Fig. 2 - LES 8/9 electrode and exhaust channel schematics showing both the original exit plane and exhaust channel extension. Note planes parallel and perpendicular to electrodes.

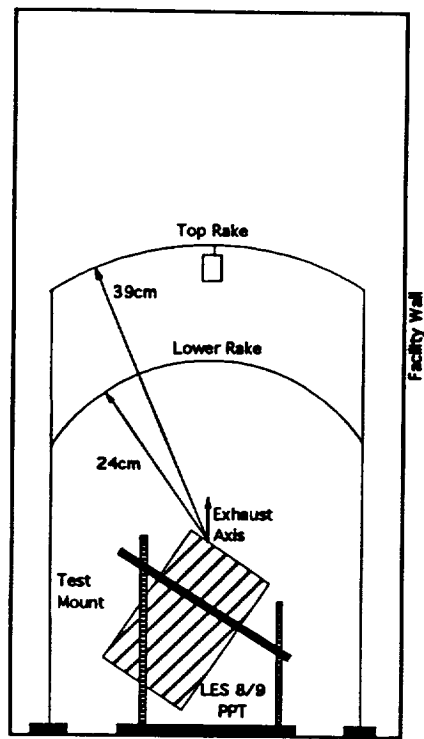


Fig. 3 - Facility used for near-field plume studies showing placement of the LES 8/9 PPT.

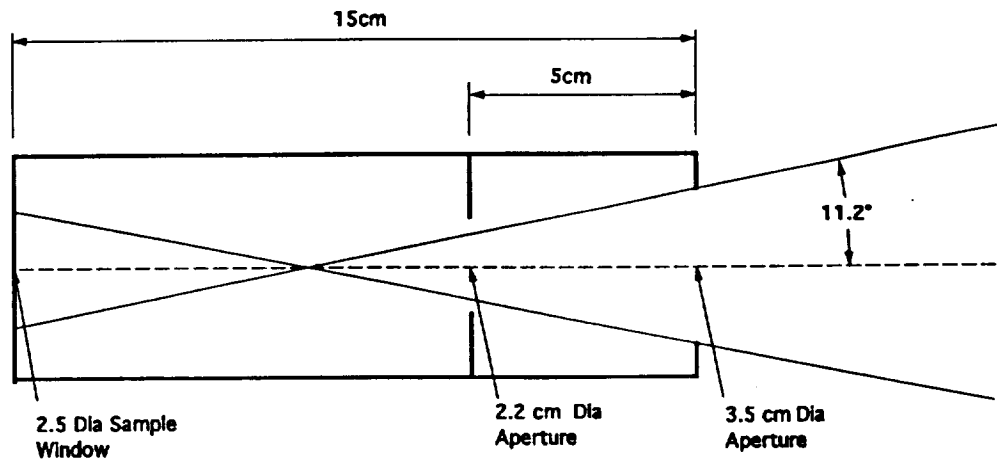


Fig. 4 - Collimators used for far-field quartz slides.

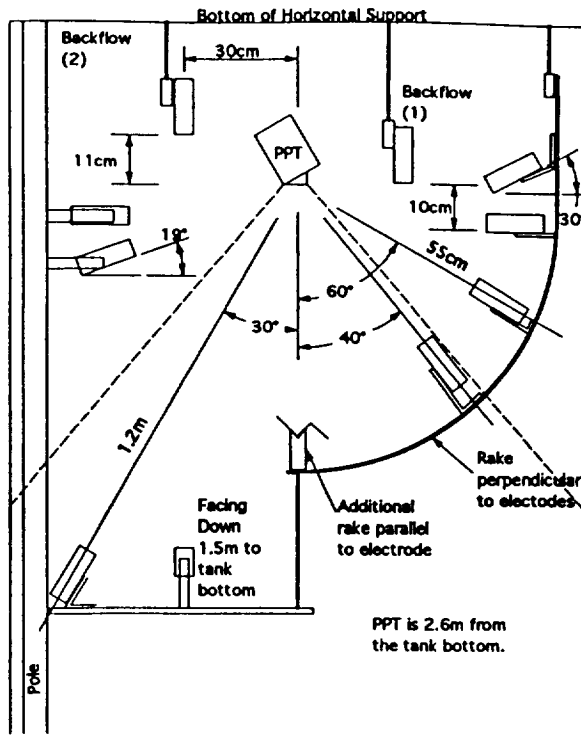


Fig 5 - Schematic of collimator positions for far-field measurements.

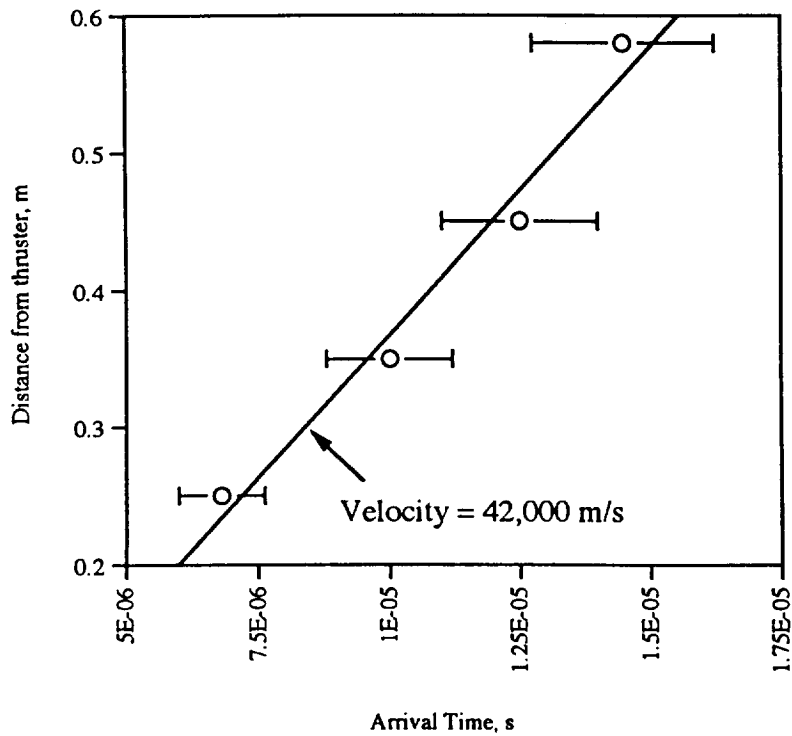
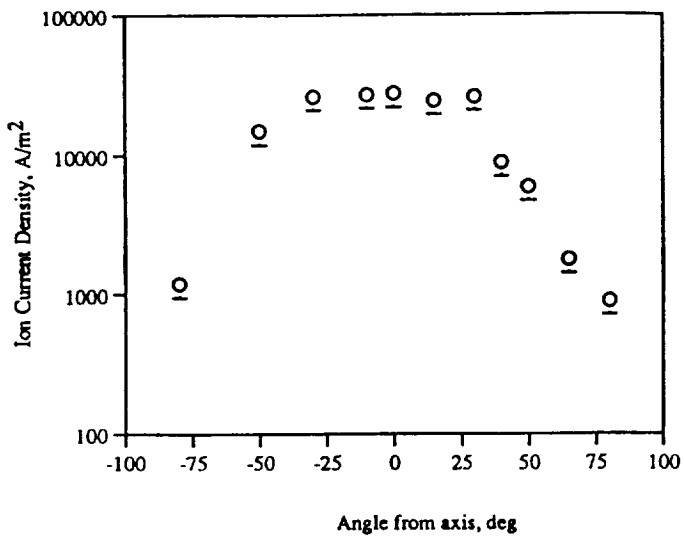
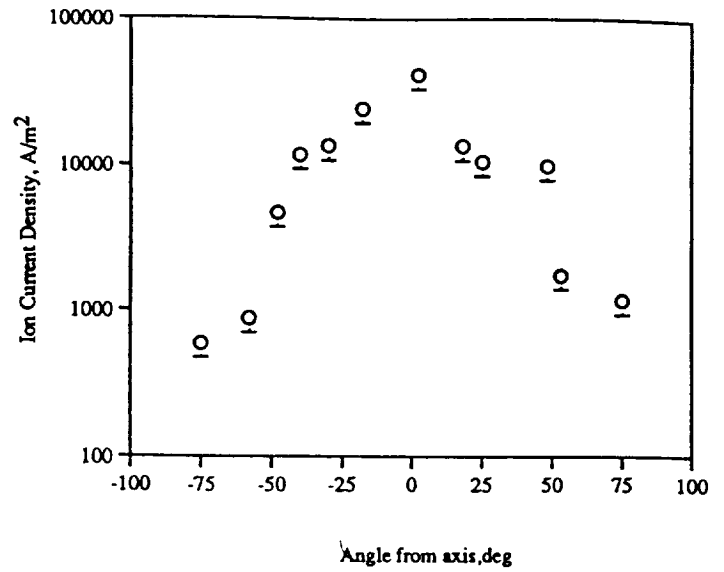


Fig 6 - Time-of-flight ion velocity measurements along plume centerline.



a. parallel to PPT electrodes.



b. perpendicular to PPT electrodes

Fig. 7 - Ion current density 24 cm from thruster.

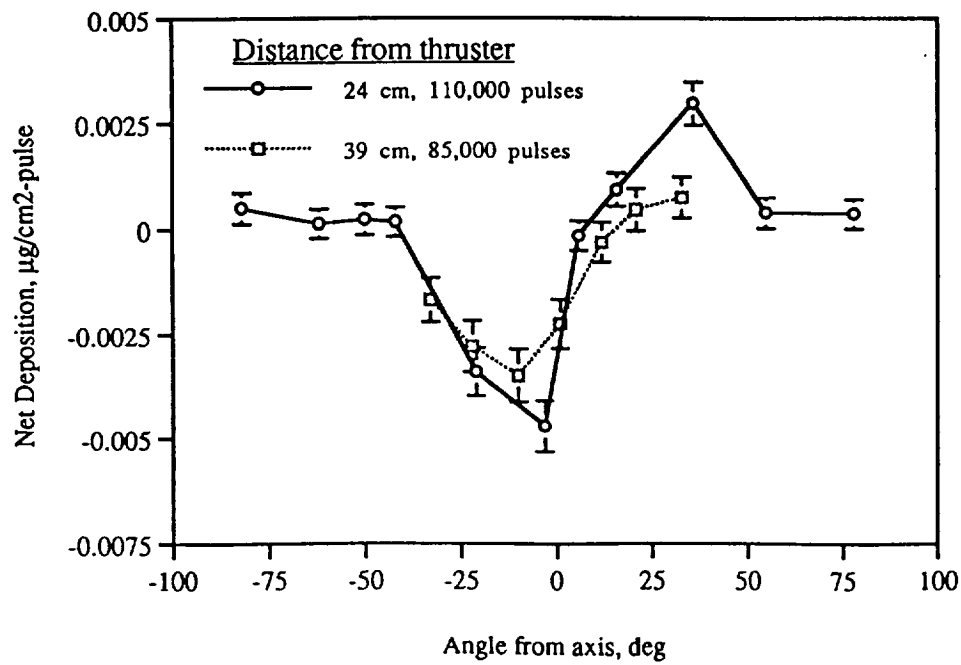


Fig. 8 - Net deposition on quartz slides in near-field region.

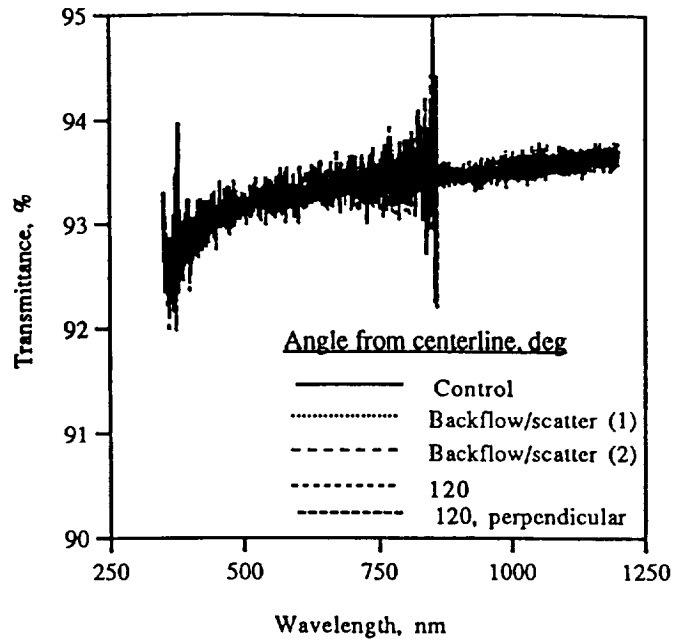
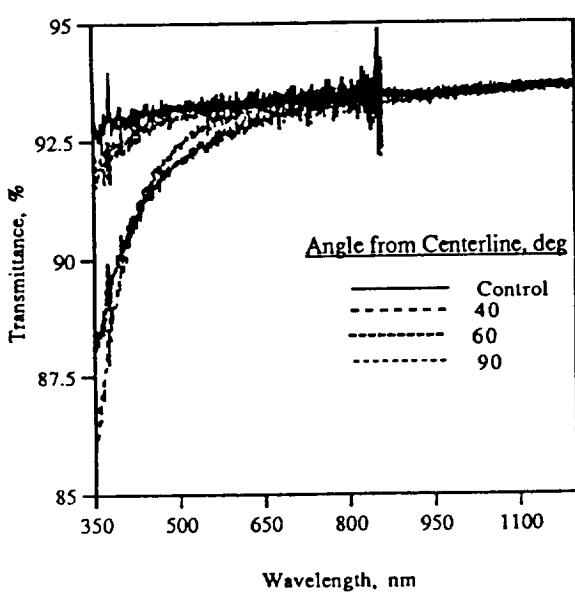
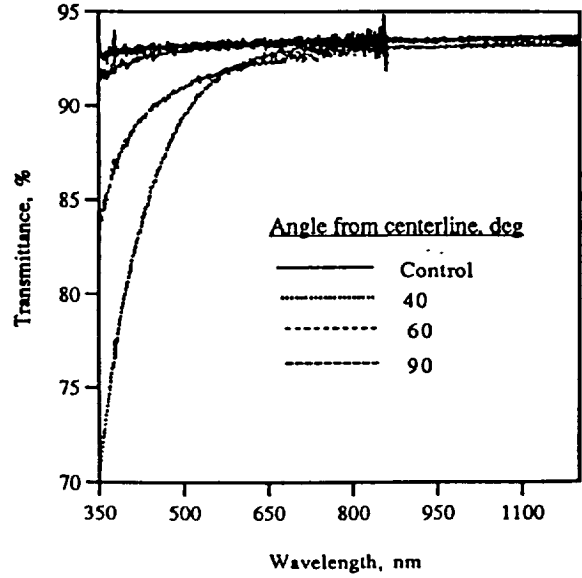


Fig. 9 - Quartz Transmittance for samples behind thruster after 2×10^5 pulses.



a. Parallel to PPT electrodes



b. Perpendicular to PPT electrodes

Fig. 10 - Quartz transmittance for samples 55 cm from thruster after 2×10^5 pulses.

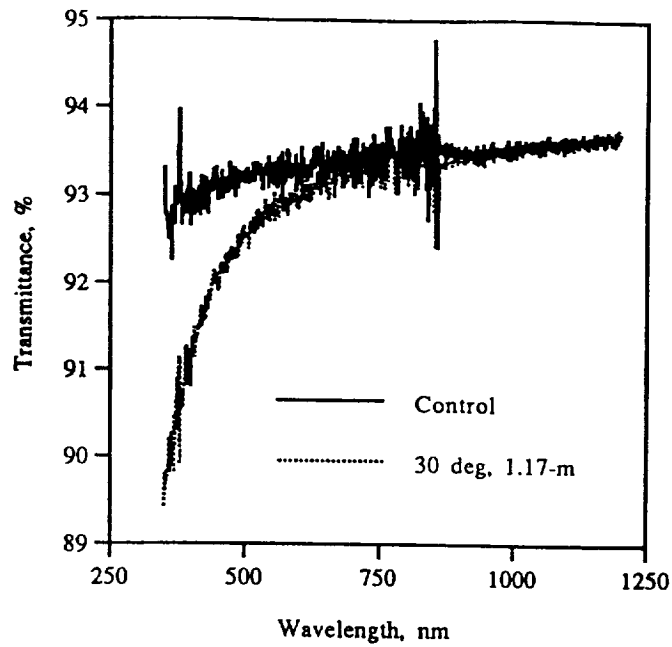


Fig. 11 - Quartz transmittance 1.2 m from thruster, 30° off-axis in plane perpendicular to PPT electrodes after 2×10^5 pulses.

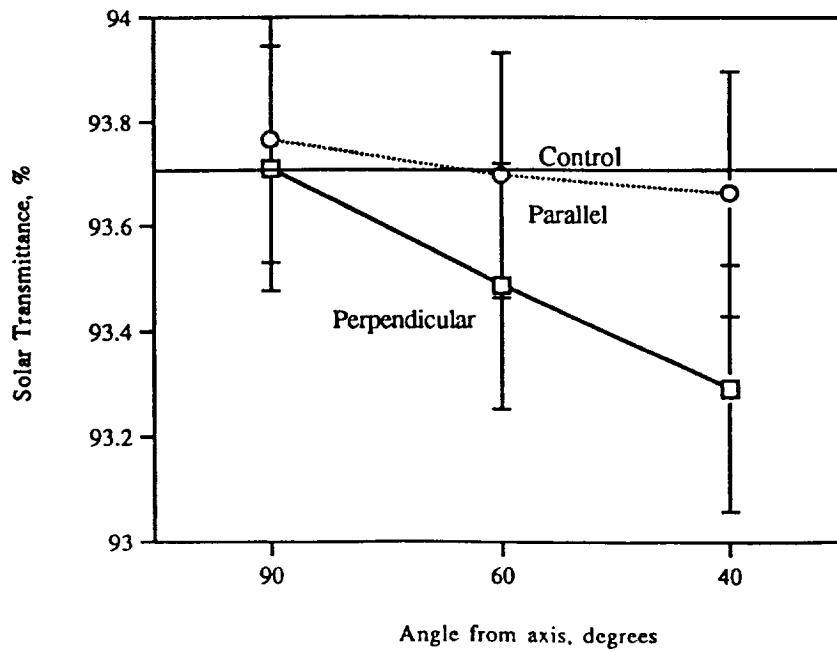


Fig. 12 - Quartz transmittance to solar radiation with samples 0.55 m from thruster in planes parallel and perpendicular to PPT electrodes after 2×10^5 pulses.

REPORT DOCUMENTATION PAGE

Form Approved
OMB No. 0704-0188

Public reporting burden for this collection of information is estimated to average 1 hour per response, including the time for reviewing instructions, searching existing data sources, gathering and maintaining the data needed, and completing and reviewing the collection of information. Send comments regarding this burden estimate or any other aspect of this collection of information, including suggestions for reducing this burden, to Washington Headquarters Services, Directorate for Information Operations and Reports, 1215 Jefferson Davis Highway, Suite 1204, Arlington, VA 22202-4302, and to the Office of Management and Budget, Paperwork Reduction Project (0704-0188), Washington, DC 20503.

1. AGENCY USE ONLY (Leave blank)	2. REPORT DATE September 1996	3. REPORT TYPE AND DATES COVERED Technical Memorandum	
4. TITLE AND SUBTITLE Pulsed Plasma Thruster Contamination		5. FUNDING NUMBERS WU-242-70-02	
6. AUTHOR(S) Roger M. Myers, Lynn A. Arrington, Eric J. Pencil, Justin Carter, Jason Heminger, and Nicolas Gatsonis		8. PERFORMING ORGANIZATION REPORT NUMBER E-10434	
7. PERFORMING ORGANIZATION NAME(S) AND ADDRESS(ES) National Aeronautics and Space Administration Lewis Research Center Cleveland, Ohio 44135-3191		10. SPONSORING/MONITORING AGENCY REPORT NUMBER NASA TM-107328 AIAA-96-2729	
9. SPONSORING/MONITORING AGENCY NAME(S) AND ADDRESS(ES) National Aeronautics and Space Administration Washington, D.C. 20546-0001		11. SUPPLEMENTARY NOTES Prepared for the 32nd Joint Propulsion Conference cosponsored by AIAA, ASME, SAE, and ASEE, Lake Buena Vista, Florida, July 1-3, 1996. Roger M. Myers and Lynn A. Arrington, NYMA, Inc., 2001 Aerospace Parkway, Brook Park, Ohio 44142 (work funded by NASA Contract NAS3-27186); Eric J. Pencil, Lewis Research Center; Justin Carter, Jason Heminger, and Nicolas Gatsonis, Worcester Polytechnic Institute; Worcester, Maine. Responsible person, Eric J. Pencil, organization code 5330, (216) 977-7463.	
12a. DISTRIBUTION/AVAILABILITY STATEMENT Unclassified - Unlimited Subject Categories 18 and 20 This publication is available from the NASA Center for AeroSpace Information, (301) 621-0390.		12b. DISTRIBUTION CODE	
13. ABSTRACT (Maximum 200 words) Pulsed Plasma Thrusters (PPTs) are currently baselined for the Air Force Mightysat II.1 flight in 1999 and are under consideration for a number of other missions for primary propulsion, precision positioning, and attitude control functions. In this work, PPT plumes were characterized to assess their contamination characteristics. Diagnostics included planar and cylindrical Langmuir probes and a large number of collimated quartz contamination sensors. Measurements were made using a LES 8/9 flight PPT at 0.24, 0.39, 0.55, and 1.2 m from the thruster, as well as in the backflow region behind the thruster. Plasma measurements revealed a peak centerline ion density and velocity of $\sim 6 \times 10^{12} \text{ cm}^{-3}$ and 42,000 m/s, respectively. Optical transmittance measurements of the quartz sensors after 2×10^5 pulses showed a rapid decrease in plume contamination with increasing angle from the plume axis, with a barely measurable transmittance decrease in the ultraviolet at 90°. No change in optical properties was detected for sensors in the backflow region.			
14. SUBJECT TERMS Pulse plasma thruster; Contamination		15. NUMBER OF PAGES 14	
		16. PRICE CODE A03	
17. SECURITY CLASSIFICATION OF REPORT Unclassified	18. SECURITY CLASSIFICATION OF THIS PAGE Unclassified	19. SECURITY CLASSIFICATION OF ABSTRACT Unclassified	20. LIMITATION OF ABSTRACT